

## Article

# Spectra of Low Energy Electrons Emitted in the Interaction of Slow Ne<sup>+</sup> Ions with Mg Surfaces

Pierfrancesco Riccardi <sup>1,\*</sup>  and Catherine A. Dukes <sup>2</sup>

<sup>1</sup> Dipartimento di Fisica, Università della Calabria and INFN Gruppo Collegato di Cosenza, Via P. Bucci Cubo 33c, 87036 Rende, Italy

<sup>2</sup> Laboratory for Astrophysics and Surface Physics, Materials Science and Engineering, University of Virginia, Charlottesville, VA 22904, USA; car8r@virginia.edu

\* Correspondence: pierfrancesco.riccardi@unical.it

**Abstract:** We measured spectra of low energy electrons emitted in the interaction of singly charged Ne<sup>+</sup> ions with the Mg surface at incident ion energies ranging from 50 eV to 4 keV. The study examines issues related to the excitation of both the surface and the bulk plasmons of the target. We will also focus on the dynamics of the production of the singlet Ne2p<sup>4</sup>(<sup>1</sup>D)3s<sup>2</sup> and triplet Ne2p<sup>4</sup>(<sup>3</sup>P)3s<sup>2</sup> autoionizing states of projectiles scattered in a vacuum. The threshold behavior of the autoionization lines show that double excitation occurs simultaneously in a single scattering. The predominant excitation of the triplet state indicates the importance of charge rearrangement and the electron correlation effects during the collisional excitation.

**Keywords:** surface scattering; autoionization and Auger processes; plasmons; electron emission



**Citation:** Riccardi, P.; Dukes, C.A. Spectra of Low Energy Electrons Emitted in the Interaction of Slow Ne<sup>+</sup> Ions with Mg Surfaces. *Surfaces* **2023**, *6*, 257–267. <https://doi.org/10.3390/surfaces6030018>

Academic Editor: Gaetano Granozzi

Received: 1 July 2023

Revised: 27 July 2023

Accepted: 1 August 2023

Published: 3 August 2023



**Copyright:** © 2023 by the authors. Licensee MDPI, Basel, Switzerland. This article is an open access article distributed under the terms and conditions of the Creative Commons Attribution (CC BY) license (<https://creativecommons.org/licenses/by/4.0/>).

## 1. Introduction

Electron emission is a fundamental consequence of the interaction of charged particles with the surfaces of solids and is of crucial importance in many applications, such as electrical discharge, spectroscopic techniques for the characterization of materials, as well as microscopy. Advances in all these research areas call for an improved understanding of electronic excitation and energy deposition and conversion processes in solids [1–3]. Two quantities are measured in studies of electron emission as a function of several variables, such as impact energy, incidence and emission angles, surface conditions, etc. These are the energy distributions of emitted electrons and their integrals, the electron emission yield. Knowledge of the yield, i.e., the number of electrons emitted per incident projectile, is generally required for these applications, while studies of the energy distribution of emitted electrons give information on specific emission phenomena, which are individuated by their characteristic spectral signatures. In the case of atomic projectiles, since they carry both potential and kinetic energy, a traditional classification divides electron emission phenomena into two main categories, namely that of potential electron emission and that of kinetic electron emission [1,4–11]. For potential electron emission (PEE) [1,4–7], the potential energy stored in the excited or ionized states of the projectiles is converted into electron excitation and emission by charge transfer processes between the projectile and the surface. The energy conversion occurs through non-local resonant and/or Auger processes that occur outside the surface and involve the electronic structure of the solid surface. Resonant charge transfer does not give origin to electron emission directly but can be the precursor of an Auger deexcitation process. Moreover, resonant processes can determine the charge and excitation state of impinging particles, which in turn determines the excitation process during a subsequent binary atomic collision. For example, according to the taxonomy introduced by Hagstrum [4], an incoming ion can be neutralized via Auger neutralization (AN), which involves two electrons from the solid surface, or via an interatomic Auger deexcitation following the resonant capture of an electron from the solid

into an excited level of the projectile. The neutralization of incoming ions can result also in plasmon excitation if sufficient potential energy is released in the electron capture from the surface. This is another important mechanism for PEE that has been investigated for free-electron metal surfaces [1,7]. The excitation of plasmons is experimentally identified by the characteristic structure that is produced in the energy distribution of emitted electrons when the plasmons decay, transferring their energy to a valence or conduction electron.

PEE occurs when the projectile is outside the surface. It depends on the distance from the surface but does not require the motion of the projectiles. However, this motion influences the process via the distance-dependent shift of the energy levels of the atomic projectile and the non-adiabaticity of the interaction with the surface. This introduces a velocity-dependent broadening of the spectra of emitted electrons [12,13]. Therefore, PEE dominates the emission at a low impact energy, while the transfer of the kinetic energy of incoming particles (kinetic electron emission—KEE) [8–11] becomes increasingly important with increasing ion energy. KEE can occur by the excitation of solid valence electrons in binary collisions with the projectiles [8]. The process occurs at impact energies larger than a threshold value, determined by energy and momentum conservation. At the impact energies of interest here, because of the large mass mismatch between the electron and the projectile, valence electron excitation is an important mechanism for light projectiles such as protons and helium [12]. For heavier particles, the threshold velocity for valence electron excitation is considerably larger and, below this threshold, KEE is determined by electron promotion [14]. In addition, electron promotion processes are characterized by sharp thresholds. However, below the threshold for promotion, electron emission does not vanish, implying the existence of other emission phenomena which are not yet understood [10].

Electron promotion [14,15] is therefore one of the main subjects of investigation of this work. It is a local process that occurs during a collision between two atoms. According to the molecular orbital model by Fano and Lichten [14,15], the collision is treated as the formation of a transient molecular system in which the energy of some molecular level increases with decreasing internuclear distance. Because of the motion of the atomic nuclei, the molecular system evolves non-adiabatically, and electrons can be transferred to higher energy levels (electron promotion) at the adiabatically forbidden crossings between molecular levels [14,15]. Electron promotion processes are usually studied by molecular orbital correlation diagrams that allow for the identification of the promoted orbitals and the threshold internuclear distance for the excitation, which is generally sharp, as experimentally verified. Therefore, electron emission is a direct consequence of electron promotion, as electrons can be directly promoted into the continuum. More important for the present study, electrons can be promoted into bound excited states above the vacuum level that decay after the collision via Auger or autoionization emission. Therefore, this emission can be revealed and studied in detail by electron spectroscopy techniques. As above mentioned, these excitations are well accounted for by the molecular orbital promotion model [14] developed for collisions in the gas phase. However, the solid nature of the target introduces new effects so that the spectra of electron emission can be quite different from those recorded in the gas phase. Therefore, the study of these excitations through electron spectroscopy [16–20] gives a deep insight into the important features of particle-solid interactions, providing additional information that can supplement those obtained by other scattering techniques, such as charge fraction and energy loss experiments, which are currently renewing interest in these processes [21–31].

Motivated by issues raised by recent research on charge exchange and energy deposition in ion scattering from solids [23–30], we have recently investigated electron emission processes in ion-surface interactions [1,16–20]. Those works focused on the interaction of noble gas and sodium ions on Al surfaces. In particular, we investigated electron promotion and its importance in the understanding of the charge state and the energy loss of projectiles scattered from the solid. In this new work we present new results obtained for the surfaces of Mg, another prototypical free-electron metal that has been investigated less than Al.

We measured the spectra of low energy electrons emitted in the interaction of 50–4000 eV  $\text{Ne}^+$  ions with atomically clean Mg surfaces. The spectra of electrons emitted from the Mg surface give insight into the mechanisms for electronic excitation and the dynamics of the electronic interactions during the scattering. The importance of this study on the magnesium target is twofold. First, we will examine plasmon excitation and decay, discussing issues that could not be addressed in studies of Al and were not resolved by previous works on Mg [32,33]. Second, we will also focus on the two features due to the decay of singlet  $2p^4(^1D)3s^2$  and triplet  $2p^4(^3P)3s^2$  autoionizing states of scattered projectiles, which are investigated at varying the incident energies of incoming ions. These excited states are produced by the simultaneous promotion of both 2p electrons in a collision involving a neutralized neon and a target atom. The study of the autoionization lines provides basic insight into details of the electronic interactions that determine collisional excitations and energy loss, an insight that cannot be achieved by other ion scattering techniques. The autoionization spectrum is dominated by the peaks due to the autoionization of the triplet state, indicating the importance of charge rearrangement and the electron correlation effects during collisional excitation. Throughout the paper we will compare the results with those obtained with the Al target, highlighting similarities and differences.

## 2. Experiments

The experiments were carried out in an ultrahigh vacuum system equipped with an ion pump that allowed us to reach an ultimate base pressure in the low  $10^{-10}$  Torr range. Singly charged neon ions are produced in an electron impact source. The discharge voltage in the source was controlled so that doubly charged  $\text{Ne}^{++}$  species do not significantly contaminate the beam [34]. The same neon beam at 4 keV was used to clean the polycrystalline Mg surface by sputtering. The sample was sputter cleaned until no oxygen and carbon signals were detected by Auger electron spectroscopy and until the ion-induced electron emission spectra became constant. The spectrometer was a cylindrical mirror analyzer that collected the electrons emitted in a cone with a semi aperture of  $43^\circ$  around the surface normal. A constant pass energy of 40 eV and a resolution of about 0.2 eV were used for the measurements of the ion-induced electron emission spectra. The spectra were measured in the 0–30 eV energy range. The transmission of the spectrometer is constant in this electron energy range. The beam impinged with an angle  $\Theta_i = 78^\circ$  measured with respect to the surface normal. The normal to the surface was parallel to the axis of the spectrometer. Under this geometry, the doppler shift and broadening of the autoionization lines of the singlet  $\text{Ne}2p^4(^1D)3s^2$  and the triplet  $\text{Ne}2p^4(^3P)3s^2$  states of neon was negligible and the lines appeared quite symmetric [16,17]. Calibration of the energy scale was achieved by imposing that the autoionization line of the triplet  $\text{Ne} 2p^4(^3P)3s^2$  state appeared at an energy of 20.35 eV, typical of the autoionization line for an isolated neon in a vacuum.

## 3. Results and Discussion

We measured the spectra of electrons emitted with energies in the range 0–30 eV by finding the impact of singly charged  $\text{Ne}^+$  ions impinging on the Mg surface at incident energies in the range from 50 eV to 4 keV and at an incidence angle  $\Theta_i = 78^\circ$ . Electrons were collected along the normal to the surface. Typical electron spectra are reported in Figure 1.

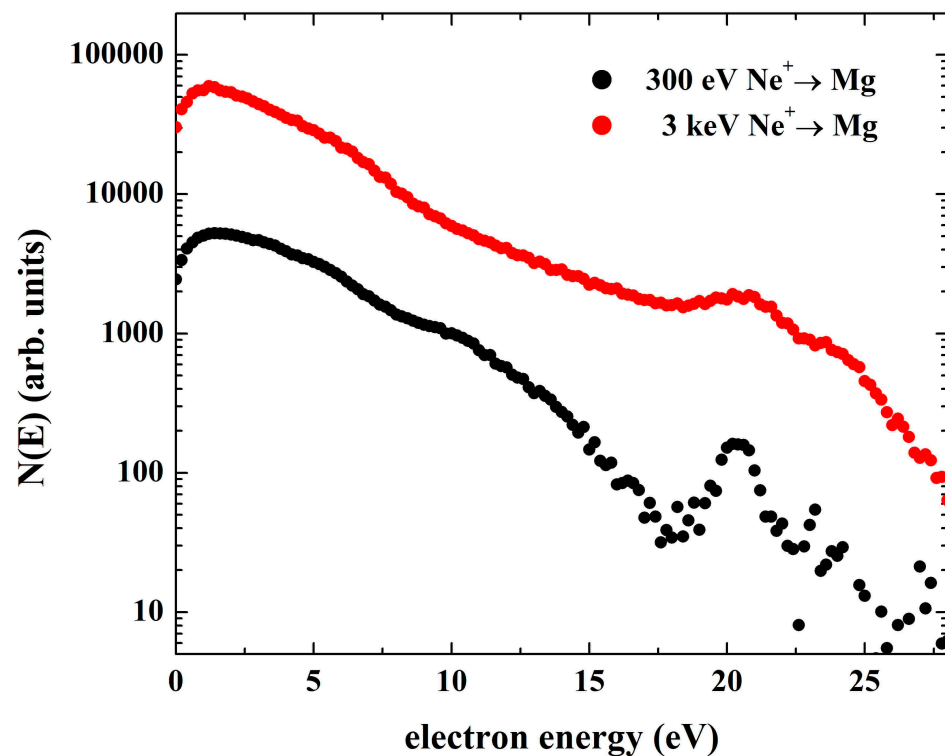


**Figure 1.**  $N(E)$ , the energy distributions of electrons emitted from Mg surfaces by 300 eV and 3 keV  $\text{Ne}^+$  ions.

### 3.1. General Features of the Spectra

The shapes of the electron spectra revealed during the interaction of 300 eV and 3000 eV  $\text{Ne}^+$  ions with the Mg surface are compared in Figure 1. The spectra are consistent with earlier measurements [7] and are shown as acquired. The spectra show several features, which are superimposed on the background of secondary electrons. To better discern these features in Figure 2, we show the numerical derivatives of the spectra in Figure 1. The derivatives were calculated with a Savitsky–Golay algorithm. A slight smoothing was applied, and care was taken so that this procedure did not introduce artifacts.

The spectrum revealed with the 300 eV neon beam shows features that are characteristic of PEE. PEE results in two broad features that are produced by the electrons emitted when the potential energy stored in the projectiles is released when they are neutralized via Auger capture or plasmon assisted neutralization. The electrons emitted by Auger neutralization can have a maximum energy (when the two electrons participating in the Auger process are at the Fermi level of the surface)  $E_b = I' - 2\Phi$  [4,7]. Here,  $I'$  is the ionization potential of the parent atom, which is reduced by an energy  $\Delta$  due to the image interaction, and  $\Phi$  is the metal work function. Given that the work function of Mg is  $\Phi = 3.75$  eV and the ionization potential of an isolated neon atom is  $I = 21.6$  eV, this emission is therefore identified by the feature revealed in the spectrum that is excited by the 300 eV  $\text{Ne}^+$  ions in the energy range 8–13 eV, which results in the minimum in the derivative  $dN(E)/dE$  in Figure 2 at the energy  $E_b \sim 12$  eV. This implies a shift of the ionization potential  $\Delta \sim 2$  eV consistent with the earlier estimations [4].

The feature revealed at a 4–8 eV energy in both spectra is assigned to the emission of electrons from the decay of plasmons [1,7]. This decay results in an electron spectrum that has a maximum energy at  $E_m = E_{pl} - \Phi$ , where  $E_{pl}$  is the plasmon energy. This edge corresponds to the minimum which is marked by the red line in the derivatives  $dN(E)/dE$  of Figure 2. For 300 eV neon projectiles, the minimum is observed at about 6 eV, which is significantly lower than the energy expected from the decay of the Mg bulk plasmon (10.6 eV minus  $\Phi = 3.75$  eV for Mg), but it is consistent with the energy expected for the multipole surface plasmon [1]. These plasmons are excited when the projectile

is still outside the surface [1,7] as a consequence of the electron capture processes that neutralize incoming (or outgoing) ions to their ground states. Differently from Al surfaces, where the structures due to AN and to the decay of plasmons are strongly overlapped and nearly undistinguishable [7], for Mg these structures are clearly distinguished because of the lower energy of the plasmon of Mg. The structure due to the decay of plasmons is clearly separated in energy from the feature due to AN (the separation being  $I' - \Phi - E_{pl}$ ). Our measurements therefore provide an unambiguous identification of both the AN and the plasmon structures, particularly the last one, that were not resolved in previous studies using helium projectiles [32].

As mentioned above, the spectrum for 300 eV neon does not reveal bulk plasmon excitation, as was theoretically proposed in the PEE regime [33]. In our experiments, bulk plasmons are revealed at higher impact energies when KEE is the dominant mechanism, as shown in the spectrum for 3 keV neon in Figure 1. KEE spectra are dominated by a broad spectrum of secondary electrons so that the plasmon dip in the derivative is less pronounced, though clearly identified. Analysis of the plasmon dips has been discussed in the case of Al samples [35]. For the Mg sample, the spectrum for 3 keV neon shows a feature that results in the dip in the derivative at an energy of about 7 eV, closely matching the energy expected for the bulk plasmon of Mg. This observation is consistent with earlier ones on Al. Therefore, we propend to assign the excitation of bulk plasmons of Mg to the energy loss suffered by fast secondary electrons, primarily the 2p Auger electrons of Mg (not shown) excited in binary atomic collisions inside the solid [1].

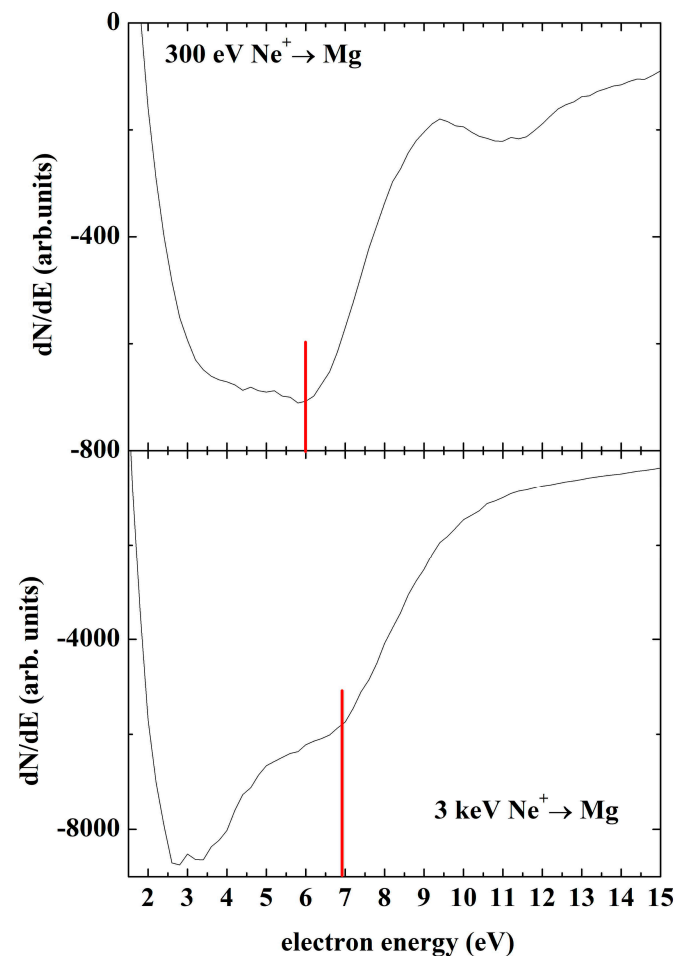


**Figure 2.** Derivative  $dN/dE$  of the spectra excited by 300 eV  $\text{Ne}^+$  (top) and 3 keV (bottom). The red line marks the position of the plasmon dips. Note the different position of the plasmon feature.

In the 18–30 eV electron energy range, both spectra in Figure 1 show two peaks due to the decay of the autoionizing triplet  $\text{Ne}[2p^4(^3P)3s^2]$  and singlet  $\text{Ne}[2p^4(^1D)3s^2]$  state of Neon [1]. These peaks are narrow, ensuring that they are produced by the decay of projectiles in a vacuum excited in a previous collision with a target atom [16–19]. These projectiles are scattered in a vacuum with holes in the 2p produced in a Ne–Al collision by the promotion of the  $4f\sigma$  molecular state, correlated to the 2p atomic orbital of the lighter element [15,20]. This process has a sharp threshold, which is evidenced by the data shown in Figure 3, reporting the threshold behavior of the autoionization lines of neon impacting Mg. The results are consistent with the threshold measured in the neon impact on Al [36].

The intensities of the autoionization lines at varying incident ion energies  $E_i$  is reported in Figure 4. The intensities have been evaluated by integrating the autoionization peaks after the normalization of the spectra to the beam current and the subtraction of a smooth background. We observe that the intensities increase with  $E_i$  while the ratio between the intensity of the triplet  $^3P$  state over the intensity of the singlet  $^1D$  state decreases with  $E_i$ .

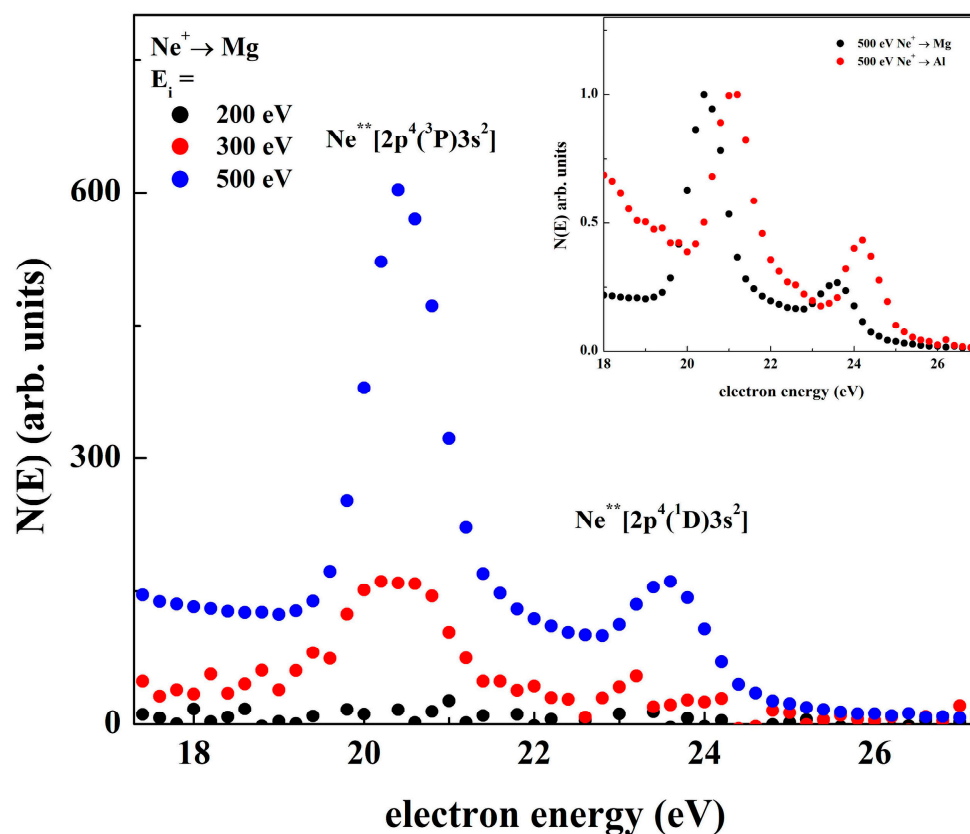


**Figure 3.** Threshold behavior of the triplet  $\text{Ne}2p^4(^3P)2s^2$  and the singlet  $\text{Ne}2p^4(^1D)2s^2$  autoionization lines. Inset: Comparison of the autoionization lines for the impact of 500 eV  $\text{Ne}^+$  on Mg and Al. The normalization to the same height shows that the intensity ratio between the triplet and the singlet line is larger for Mg. The different position of the spectra is due to the different work function of Al and Mg [37].

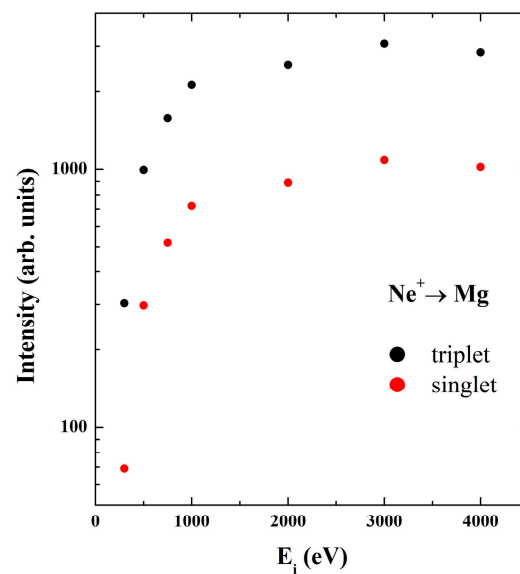


**Figure 4.** Dependence on impact energy  $E_i$  of the intensities of the triplet  $\text{Ne}2p^4(^3P)2s^2$  and the singlet  $\text{Ne}2p^4(^1D)2s^2$  autoionization lines.

### 3.2. $2p^4$ Excitation of Scattered Projectiles

The common heuristic approach to discussing the electronic interaction of the projectile with the target is to divide the trajectory of the ions into three segments, separating non-local interactions with the surface, during the incoming and the outgoing trajectories (the first and the third segment), from the excitations that occur in local interactions during binary collisions (the second segment).

In the first segment, non-local interactions lead to the efficient neutralization of incoming ions [37–40]. Two mechanisms, which are clearly resolved in our spectra, contribute to the neutralization of  $\text{Ne}^+$ , Auger neutralization, and plasmon-assisted neutralization. Resonant processes into excited states of the projectiles may be possible and may be followed by an Auger deexcitation process leading to electron emission; this, however, is expected to be quite weak as it does not produce a clear signature in the spectra. Moreover, as they further approach the surface, the projectiles that have undergone a resonant neutralization into excited states can be ionized again via a resonant electron transfer to the surface. This complex sequence of non-local charge exchange processes determines the electronic configuration of the projectiles, which is important for the subsequent atomic collision because electron promotion processes depend critically on the charge and excitation state of colliding particles [18]. Neutralization processes are very efficient at low impact energies as their probabilities decrease with impact energy [17]. Previous results have shown that, in the investigated ion energy range, neutralization to the ground state is dominant, while only a few percent of the projectiles remain ionized [37–40]. This is consistent with our observation that the autoionization spectrum of neon is dominated by the  $2p^4$  features. The  $2p$  excitation in Ne occurs during the second step by electron promotion. The observation of the threshold behavior of these excitations in Figure 3 is consistent with the previous results obtained for Ne-Al and Na-Al [16,36] and ensures the simultaneous excitation of both  $2p$  electrons of a neutralized neon during a single scattering [16]. The result excludes the one-electron promotion and reionization model often invoked [23,24,41,42], particularly discussion of the  $2p$  excitation in Ne-Mg collision [41,42]. The model considers that, for atomic collisions in a solid, only one electron is promoted and delocalized into the continuum of the conduction band. When the projectiles move away from the surface, non-local charge exchange can occur again. This charge exchange can proceed via resonant mechanisms that can populate high-lying excited states, or via Auger or plasmon assisted processes that can change the  $2p$  configuration of scattered particles. Ultimately, the complex sequence of charge exchange and electronic excitation during the three segments results in a variety of

2p excited states that autoionize producing several peaks [37–39], dominated by the singlet and the triplet lines investigated here.

In the foregoing discussion, the second step (the binary collision) has been treated as a pure atomic collision, exactly like in the gas phase. However, our spectra also indicate that the solid nature of the target is important in determining the electronic interactions and charge exchange that occur during the collisions. A clear indication of this fact is the prominence of the triplet peak.

The excitation of the  $^3P$  state is not predicted by the MO promotion model, which predicts only the excitation of the singlet  $^1D$  through the promotion of the  $4f\sigma$  molecular orbital. Indeed, the triplet peak is very weak for collisions in the gas-phase. This weak excitation has been ascribed to the conversion of the singlet excitation into the triplet one through an Auger rearrangement mechanism during the collision [43]. This process involves the recombination of one of the two holes in the  $4f\sigma$  molecular orbital by an electron from a Rydberg molecular state. The energy in this transition is released to an electron in the  $3d\pi$  state that is excited to a higher lying state. In a solid, this two-electron transition can involve electrons from the valence band. Therefore, because of the large number of valence electrons that can be involved, it has been argued that the low probability for this process can be enhanced for collisions in solids [19,37].

On the other hand, other mechanisms that have been invoked to interpret the dominance of the triplet peak can be excluded. In the one-electron reionization mechanism [41], the intense emission from the triplet state can be explained only if the collision involves a singly charged neon with a hole in the 2p state correlated to the  $3d\pi$  MO. The promotion of one  $4f\sigma$  electron during the collisions involving these ions in this particular configuration leads to the triplet configuration. Therefore, according to the reionization model, the dominance of the triplet peak should not be observed for neutral projectiles, which is in striking contrast with the experiment performed [37–39] using  $Ne^0$  neutrals in which the intensity of the triplet peak was similar to that measured under the  $Ne^+$  impact.

Furthermore, charge exchange during the outgoing trajectory has been invoked as a possible mechanism for the production of the triplet state. These processes include atomic Auger deexcitation, Auger neutralization of  $Ne^+ 2p^3nl'n'l'$  or resonant autoionization of excited projectiles [39]. However, all these processes should be strongly dependent on the value of the work function of the surface. In contrast, the ratio between the intensities of the triplet and the singlet lines resulted were independent of the variations in the work function when Cs atoms were adsorbed on Al and other targets. Moreover, since the neon projectiles cannot be excited in collisions with Cs atoms, but only with Al because of the large mass difference, the independence of the intensity ratio when the macroscopic work function of the sample is varied implies that the process is local and related to the electronic properties close to the site of the collisional excitation [19,44].

The observation in Figure 4 that the intensity ratio between the triplet and the singlet state decreases with  $E_i$ , coupled with a decrease in this ratio with the incidence angle  $\Theta_i$  observed for Al samples [19], indicates that the process depends on the interaction time during the collision. This is consistent with the simulations that showed the lower efficiency of the conversion from the singlet to the triplet excitation for projectiles scattered with larger velocities [38].

This observation fits with the mechanism of the two-electron Auger rearrangement proposed for gas phase collisions [43]. This process occurs during the collision and involves the molecular orbitals of the transient quasi-molecular system, showing the importance of electron correlation effects occurring on a sub-femtosecond scale during the collision because of electron-electron interactions leading to two electron transitions [1,45–47]. It is energetically allowed when the internuclear distance is larger than about 2 a.u., when the  $3d\pi^4$  configuration is below the  $3d\pi^34f\sigma^1$ . As above mentioned, the calculated cross sections of the Auger rearrangement process are low in the gas phase [43]. However, it has been argued that in the solid phase there is a large number of electrons that can participate, which can enhance the process. These electrons are those in the valence band within 3.2 eV

below the Fermi level (corresponding to the energy difference between the singlet and the triplet states). The proposed Auger rearrangement is also consistent with the observation reported in the inset of Figure 3. For Mg, the intensity ratio between the singlet and the triplet peak is larger than Al. This is due to the larger mass of Al, which implies smaller impact parameters for the Ne-Al than the Ne-Mg collisions. Collisions with Al result in larger scattering angles and lower velocities of scattered Neon.

#### 4. Conclusions

In conclusion, we reported on the measurements of the energy distributions of electrons emitted by the interaction of low-energy singly charged neon ions with Mg surfaces. The study focused on plasmon excitation and projectile autoionization. Unlike for Al samples, the spectra for Mg show unambiguous signatures of plasmon excitation, clearly separated in energy from the AN ones. At a low energy  $E_i$  of the incident ions, surface plasmons are excited by PEE during the neutralization of incoming ions, while at a higher  $E_i$  bulk plasmons are excited by the transfer of the kinetic energy of incoming projectiles. The excitation of bulk plasmons by potential energy transfer, as theoretically proposed, has not been observed.

We have investigated the formation using the electron promotion of the triplet  $\text{Ne}2p^4(^3P)3s^2$  and the singlet  $\text{Ne}2p^4(^1D)3s^2$  autoionizing states of projectiles scattered in a vacuum. The threshold behavior of these lines ensures that the double excitation is produced simultaneously in a single scattering. Besides the local description of the collisional excitation process, the formation of the autoionizing states in the atomic collisions in solids requires a consideration of non-local charge exchange in both the incoming and the outgoing trajectories of the projectiles, and of the electron correlation effects that determine the dominant excitation of the triplet state. These last phenomena have been poorly investigated and electron spectroscopy represents a suited technique capable of providing deep insight into these processes. Our results show the importance of properly considering these effects for an accurate description of the dynamics of the electronic interactions during the scattering at solid surfaces, which is relevant also to other techniques of ion scattering such as charge fraction experiments and energy deposition.

**Author Contributions:** P.R.: Conceptualization, Methodology, Investigation, Writing—original draft Writing—review & editing. C.A.D.: Software, Methodology, Investigation, Data curation, Visualization. Writing—review & editing. All authors have read and agreed to the published version of the manuscript.

**Funding:** This research received no external funding.

**Institutional Review Board Statement:** Not applicable.

**Informed Consent Statement:** Not Applicable.

**Data Availability Statement:** Data are available upon reasonable request.

**Conflicts of Interest:** The authors declare no conflict of interest.

#### References

1. Riccardi, P. Electron Spectroscopy of Charge Exchange Effects in Low Energy Ion Scattering at Surfaces: Case Studies of Heavy Ions at Al Surface. *Surfaces* **2023**, *6*, 64. [[CrossRef](#)]
2. Han, W.; Zheng, M.; Banerjee, A.; Luo, Y.Z.; Shen, L.; Khursheed, A. Quantitative material analysis using secondary electron energy spectromicroscopy. *Sci. Rep.* **2020**, *10*, 22144. [[CrossRef](#)] [[PubMed](#)]
3. Fairchild, A.J.; Chirayath, V.A.; Sterne, P.A.; Gladen, R.W.; Koymen, A.R.; Weiss, A.H. Direct evidence for low-energy electron emission following O LVV Auger transitions at oxide surfaces. *Sci. Rep.* **2020**, *10*, 17993. [[CrossRef](#)]
4. Hagstrum, H.D. Low energy de-excitation and neutralization processes near surfaces. In *Inelastic Ion-Surface Collisions*; Tolk, N.H., Tully, J.C., Heiland, W., White, C.W., Eds.; Academic Press: New York, NY, USA, 1977; Volume 1.
5. Monreal, R. Auger Neutralization and Ionization Processes for Charge Exchange between Slow Noble Gas Atoms and Solid Surfaces. *Prog. Surf. Sci.* **2014**, *89*, 80. [[CrossRef](#)]
6. Baragiola, R.A. Electron Emission from Slow Ion-Solid Interactions. In *Low Energy Ion-Surface Interactions*; Rabalais, J.W., Ed.; Wiley: New York, NY, USA, 1994; Chapter 4.

7. Baragiola, R.A.; Monreal, R.C. Electron Emission from Surfaces Mediated by Ion-Induced Plasmon Excitation. In *Slow Heavy-Particle Induced Electron Emission from Solid Surfaces*; Springer Tracts in Modern Physics; Springer: Berlin/Heidelberg, Germany, 2007; Volume 225.
8. Winter, H.; Lederer, S.; Winter, H. Fermi Momentum Above Metal Surfaces from Electrons Ejected by Impact of He Ions. *Europhys. Lett.* **2006**, *75*, 964. [[CrossRef](#)]
9. Rabalais, J.; Bu, H.; Roux, C. Impact-Parameter Dependence of Ar<sup>+</sup>-Induced Kinetic Electron Emission from Ni(110). *Phys. Rev. Lett.* **1992**, *69*, 1391. [[CrossRef](#)] [[PubMed](#)]
10. Lorincik, J.; Sroubek, Z.; Eder, H.; Aumayr, F.; Winter, H. Kinetic Electron Emission from Clean Polycrystalline Gold Induced by Impact of Slow C<sup>+</sup>, N<sup>+</sup>, O<sup>+</sup>, Ne<sup>+</sup>, Xe<sup>+</sup>, and Au<sup>+</sup> Ions. *Phys. Rev. B* **2000**, *62*, 16116. [[CrossRef](#)]
11. Lederer, S.; Maass, K.; Blauth, D.; Winter, H.; Winter, H.P.; Aumayr, F. Kinetic electron emission from the selvage of a free-electron-gas metal. *Phys. Rev. B* **2003**, *67*, 121405. [[CrossRef](#)]
12. Monreal, R.; Apell, S.P. Magic energies in Auger electron spectra Nucl. Instr. Meth. Phys. Res. B **1993**, *83*, 459. [[CrossRef](#)]
13. Hagstrum, H.D.; Takeishi, Y.; Pretzer, D.D. Energy Broadening in the Auger-Type Neutralization of Slow Ions at Solid Surfaces. *Phys. Rev.* **1965**, *139*, A526. [[CrossRef](#)]
14. Fano, U.; Lichten, W. Interpretation of Ar<sup>+</sup>-Ar Collisions at 50 keV. *Phys. Rev. Lett.* **1965**, *14*, 627. [[CrossRef](#)]
15. Barat, M.; Lichten, W. Extension of the Electron-Promotion Model to Asymmetric Atomic Collisions. *Phys. Rev. A* **1972**, *6*, 211–229. [[CrossRef](#)]
16. Runco, D.; Riccardi, P. Single Versus Double 2p Excitation in Neon Projectiles Scattered from Surfaces. *Phys. Rev. A* **2021**, *104*, 042810. [[CrossRef](#)]
17. Runco, D.; Riccardi, P. Collisional excitation in Neon-like projectiles scattered from Al. *Solid State Commun.* **2021**, *340*, 114534. [[CrossRef](#)]
18. Runco, D.; Riccardi, P. Charge and excitation state of Na projectiles scattered from Al surfaces. *Radiat. Eff. Defects Solids* **2021**, *176*, 995–1002. [[CrossRef](#)]
19. Riccardi, P.; Dukes, C.A. Excitation of the Triplet 2p<sup>4</sup>(3P)3s<sup>2</sup>Autoionizing State of Neon by Molecular Orbital Electron Promotion at Solid Surfaces. *Chem. Phys. Lett.* **2022**, *798*, 139610. [[CrossRef](#)]
20. Riccardi, P.; Dukes, C. Effects of the solid target on electronic excitations during binary atomic collisions in the interaction of Ne ions with Al surfaces. *Vacuum* **2022**, *204*, 111393. [[CrossRef](#)]
21. Lohmann, S.; Holeňák, R.; Grande, P.L.; Primetzhofer, D. Trajectory dependence of electronic energy-loss straggling at keV ion energies. *Phys. Rev. B* **2023**, *107*, 085110. [[CrossRef](#)]
22. Ntemou, E.; Lohmann, S.; Hohenák, R.; Primetzhofer, D. Electronic interaction of slow hydrogen, helium, nitrogen, and neon ions with silicon. *Phys. Rev. B* **2023**, *107*, 155145. [[CrossRef](#)]
23. Lohmann, S.; Holeňák, R.; Primetzhofer, D. Trajectory-dependent electronic excitations by light and heavy ions around and below the Bohr velocity. *Phys. Rev. A* **2020**, *102*, 062803. [[CrossRef](#)]
24. Lohmann, S.; Primetzhofer, D. Disparate Energy Scaling of Trajectory-Dependent Electronic Excitations for Slow Protons and He Ions. *Phys. Rev. Lett.* **2020**, *124*, 096601. [[CrossRef](#)] [[PubMed](#)]
25. Hohenak, R.; Lohman, S.; Sekula, F.; Primetzhofer, D. Simultaneous Assessment of Energy, Charge State and Angular Distribution for Medium Energy Ions Interacting with Ultra-Thin Self-Supporting Targets: A time-of-Flight Approach. *Vacuum* **2021**, *185*, 109988. [[CrossRef](#)]
26. Ntemou, E.; Holeňák, R.; Primetzhofer, D. Energy deposition by H and He ions at keV energies in self-supporting, single crystalline SiC foils. *Radiat. Phys. Chem.* **2022**, *194*, 110033. [[CrossRef](#)]
27. Valpreda, A.; Sturm, J.M.; Yakshin, A.E.; Ackermann, M. Resolving buried interfaces with low energy ion scattering. *J. Vac. Sci. Technol. A* **2023**, *41*, 043203. [[CrossRef](#)]
28. Mousley, M.; Tabean, S.; Bouton, O.; Hoang, Q.H.; Wirtz, T.; Eswara, S. Scanning Transmission Ion Microscopy Time-of-Flight Spectroscopy Using 20 keV Helium Ions. *Microsc. Microanal.* **2023**, *29*, 563–573. [[CrossRef](#)]
29. Liu, P.; Yin, L.; Zhang, Z.; Ding, B.; Shi, Y.; Li, Y.; Zhang, X.; Song, X.; Guo, Y.; Chen, L.; et al. Anomalous Neutralization Characteristics in Na<sup>+</sup> Neutralization on Al(111) Surfaces. *Phys. Rev. A* **2020**, *101*, 032706. [[CrossRef](#)]
30. Wei, M.; Wang, X.; Guo, X.; Liu, P.; Ding, B.; Shi, Y.; Song, X.; Wang, L.; Liu, X.; Yin, L.; et al. Low-energy Na<sup>+</sup> neutralization on Al(1 1 1) and Cu(1 1 0) surfaces at grazing incidence. *Nucl. Instrum. Methods Phys. Res. Sect. B Beam Interact. Mater. At.* **2020**, *478*, 239–243. [[CrossRef](#)]
31. Li, S.-M.; Mao, F.; Zhao, X.-D.; Li, B.-S.; Jin, W.-Q.; Zuo, W.-Q.; Wang, F.; Zhang, F.-S. First-principles study of the electronic stopping power of indium for protons and He ions. *Phys. Rev. B* **2021**, *104*, 214104. [[CrossRef](#)]
32. Lancaster, J.C.; Kontur, F.J.; Walters, G.K.; Dunning, F.B. Neutralization of low-energy He<sup>+</sup> ions at a magnesium surface. *Nucl. Instrum. Methods B* **2007**, *256*, 37. [[CrossRef](#)]
33. Gutierrez, F.A.; Salas, C.; Jouin, H. Bulk plasmon induced ion neutralization near metal surfaces. *Surf. Sci.* **2012**, *606*, 1293. [[CrossRef](#)]
34. Mandarino, N.; Zoccali, P.; Oliva, A.; Camarca, M.; Bonanno, A.; Xu, F. Near-threshold behavior of the 2p-electron excitation in Mg-Mg, Al-Al, and Si-Si symmetric collisions. *Phys. Rev. A* **1993**, *48*, 2828. [[CrossRef](#)]
35. Stolterfoht, N.; Bremer, J.H.; Hoffmann, V.; Rösler, M.; Baragiola, R.; de Gortari, I. Mechanism for plasmon production by hollow atoms above and below an Al surface. *Nucl. Instrum. Methods B* **2001**, *182*, 89. [[CrossRef](#)]

36. Riccardi, P.; Cosimo, F.; Sindona, A. Absence of Reionization in Low Energy Na<sup>+</sup> scattering from Al Surfaces. *Phys. Rev. A* **2018**, *97*, 032703. [[CrossRef](#)]
37. Zampieri, G.; Meier, F.; Baragiola, R. Formation of autoionizing states of Ne in collisions with surfaces. *Phys. Rev. A* **1984**, *29*, 116–122. [[CrossRef](#)]
38. Xu, F.; Mandarino, N.; Oliva, A.; Zoccali, P.; Camarca, M.; Bonanno, A.; Baragiola, R.A. Projectile L<sub>2,3</sub>-Shell Electron Excitation in Slow Ne<sup>+</sup>-Al Collisions. *Phys. Rev. A* **1994**, *50*, 4040. [[CrossRef](#)] [[PubMed](#)]
39. Guillemot, L.; Lacombe, S.; Tuan, V.; Esaulov, V.; Sanchez, E.; Bandurin, Y.; Dashchenko, A.; Droblich, V. Dynamics of excited state production in the scattering of inert gas atoms and ions from Mg and Al surfaces. *Surf. Sci.* **1996**, *365*, 353–373. [[CrossRef](#)]
40. Beckschulte, M.; Taglauer, E. The influence of work function changes on the charge exchange in low-energy ion scattering. *Nucl. Instrum. Methods* **1993**, *78*, 29–37. [[CrossRef](#)]
41. Souda, R.; Yamamoto, K.; Hayami, W.; Aizawa, T.; Ishizawa, Y. Band Effect on Inelastic Rare Gas Collisions with Solid Surfaces. *Phys. Rev. Lett.* **1995**, *75*, 3552–3555. [[CrossRef](#)]
42. Souda, R.; Yamamoto, K.; Hayami, W.; Aizawa, T.; Ishizawa, Y. Low-energy He and Ne scattering from Al(111): Reionization versus autoionization. *Surf. Sci.* **1996**, *363*, 139–144. [[CrossRef](#)]
43. Østgaard-Olsen, J.; Andersen, T.; Barat, M.; Courbin-Gaussorgues, C.; Sidis, V.; Pommier, J.; Agusti, J.; Russek, A. Excitation and Charge Transfer in Low-Energy Na<sup>+</sup>-Ne Collisions. *Phys. Rev. A* **1979**, *19*, 1457. [[CrossRef](#)]
44. Bonanno, A.; Zoccali, P.; Xu, F. Ne autoionization electron emission in collisions with clean and Cs and Na covered Mg, Al, and Si surfaces. *Phys. Rev. B* **1994**, *50*, 18525. [[CrossRef](#)] [[PubMed](#)]
45. Stolterfoht, N. Evidence for autoexcitation producing inner-shell vacancies in slow ion-atom collisions. *Phys. Rev. A* **1993**, *47*, R763–R766. [[CrossRef](#)] [[PubMed](#)]
46. Riccardi, P.; Sindona, A.; Dukes, C.A. Double electron excitation in He ions interacting with an aluminum surface. *Phys. Rev. A* **2016**, *93*, 042710. [[CrossRef](#)]
47. Riccardi, P.; Dukes, C. 2p excitation in target atoms in the interaction of slow ions with Al surfaces. *Surf. Sci.* **2022**, *719*, 122025. [[CrossRef](#)]

**Disclaimer/Publisher's Note:** The statements, opinions and data contained in all publications are solely those of the individual author(s) and contributor(s) and not of MDPI and/or the editor(s). MDPI and/or the editor(s) disclaim responsibility for any injury to people or property resulting from any ideas, methods, instructions or products referred to in the content.